ELSEVIER

Engineering Structures 24 (2002) 151–162

ENGINEERING STRUCTURES

www.elsevier.com/locate/engstruct

Finite element failure analysis of reinforced concrete T-girder bridges

Ha-Won Song [a,*], Dong-Woo You [1,a], Keun-Joo Byun [a], Koichi Maekawa [b]

[a] *Department of Civil Engineering, Yonsei University, Seoul, South Korea*
[b] *Department of Civil Engineering, University of Tokyo, Tokyo, Japan*

Received 25 January 2001; received in revised form 12 September 2001; accepted 14 September 2001

Abstract

Failure behaviors of in-situ deteriorated reinforced concrete T-girder bridges under cyclic loading is experimentally observed and a finite element modeling technique to predict the behaviors is developed. In this study, full-scale destructive tests of in-situ bridges are performed by applying cyclic loads up to failure, and modeling techniques for the non-linear finite element analysis of in-situ deteriorated reinforced concrete T-girder bridge are presented. Two in-situ reinforced concrete T-girder bridges were selected for the failure tests and the analysis, one a symmetrically loaded bridge and the other a non-symmetrically loaded bridge. Path-dependent in-plane constitutive laws of cracked reinforced concrete were utilized for material modeling of the analysis. An RC zoning method was applied to two-dimensional finite element modeling of the symmetrically loaded bridge and a combination of frame elements utilizing the fiber technique and layered shell elements were used for three-dimensional modeling of the non-symmetrically loaded bridge. Experimental results indicate that significant load carrying capacity is retained in old reinforced concrete bridges and analysis results show that the manner of modeling of degraded support conditions significantly affects the predicted responses of the capacity as well as the stiffness of the bridges. This significant effect of support conditions of the deteriorated RC bridges is verified and a simple modeling technique for the support condition is proposed to consider the degradation of supports. By applying the proposed modeling to the boundary condition of the bridges, a finite element failure analysis is carried out for the bridges subjected to cyclic loading. Then, the analytical results are compared with full-scale failure test results. The comparison shows that the finite element analysis technique along with the proposed boundary condition can be effectively applied to the failure analysis of in-situ reinforced concrete T-girder bridges subjected to cyclic loading.

Keywords: Full-scale failure test; Reinforced concrete T-girder bridges; Finite element analysis; Cyclic loading; Load carrying capacity; Support condition modeling

1. Introduction

Field tests of in-situ bridges can be either destructive or non-destructive. Destructive failure tests are those in which the bridge is loaded until failure occurs. The main objective of destructive tests is to gain insight into the ultimate load-carrying capacity of bridges. A survey of destructive tests of old bridges [6,9] reveals that most reinforced concrete bridges possess significant reserve strength despite their already deteriorated conditions, which are not predicted by conventional analytical models. In particular, the effects of support conditions and non-structural elements like the curbs of aged bridge were found to be considerable [7]. Even though non-linear analyses of reinforced concrete structures have shown significant improvements during the past three decades, most efforts in non-linear finite element analysis have focused on simulating the responses of individual elements or simple structural assemblages and verifying the results based on experimental data. Through continued efforts to overcome these limitations, the technique for proper non-linear analysis of complete reinforced concrete frame structures appears to be well established now [7,18]. However, full-scale destructive field tests on in-situ bridges focused on strength and stiffness characteristics of aged reinforced concrete

* Corresponding author. Tel.: +82-2-2123-2806; fax: +82-2-364-5300.
E-mail address: song@yonsei.ac.kr (H.-W. Song).
[1] At present Senior Researcher of Korea Infrastructure Safety and Technology Corporation.

0141-0296/02/$ - see front matter
PII: S0141-0296(01)00107-9

bridges subjected to cyclic loading up to failure are rare, and finite element failure analyses focused on the degradation of support conditions and cyclic behaviors of the bridges are even rarer.

In this paper, two in-situ aged reinforced concrete T-girder bridges are selected for cyclic failure tests and finite element analysis. Full-scale destructive tests are carried out by imposing cyclic load either symmetrically or non-symmetrically. The bridge's monotonic behaviors both at service and ultimate load levels are observed and used to construct a simple modeling technique for the support condition, which found to be significant in the analysis. Two- and three-dimensional finite element modeling techniques for symmetrically and non-symmetrically loaded bridges, respectively, and constitutive laws of cracked reinforced concrete are described. Finally, finite failure analysis is carried out for the two T-girder bridges and their obtained cyclic responses are compared with the results obtained from the full-scale destructive failure tests.

2. Target bridges

The target RC bridges for failure analysis and experiment are two reinforced concrete T-girder bridges decommissioned for several years; one is about 50 years old and was decommissioned in 1981, while the other is about 40 years old and was decommissioned in 1993.

The 50-year old reinforced concrete T-girder bridge comprises eleven, cast-in-place, simple supported spans, with three T-girders for each 12 m span designed for DB 13.5 ton (132.3 kN) [1] with a two-lane roadway. Although the superstructure of the bridge is in a relatively good condition, the bridge was decommissioned in 1981 due to severe damage to its piers. A general condition survey indicates that the girders of the bridge are still in good condition with the exception of small cracks and minor spallings, but major damage in the superstructure is concentrated on the rails and curbs. Since the concrete quality of the third span is better than that of the others and the test conditions, including installation of ground anchors for loading, for the third span are good, the third span of the bridge was selected for a full-scale destructive test and failure analysis. Fig. 1 shows the dimensions of the T-girder section of the bridge. For a destructive test of the bridge subjected to symmetric loading, the flange of the third span of the bridge was cut longitudinally to make an idealized single T-girder bridge. The reinforcement layout of the single span first target bridge is illustrated in Fig. 2. Based on standard tests conducted on cores taken from the flange of the third span and reinforcing bar samples taken from the webs of the third span upon completion of the test, the basic material properties of the bridge were determined. The average values of the measured initial elastic modulus of concrete and the compressive strength are 26,470 and 35.3 MPa, respectively; the yield stress of the reinforcement bar is 435.8 MPa.

The second target bridge is a cast-in-place, 9.2 m simple supported RC T-girder bridge. Fig. 3 shows the dimensions of the RC T-girder with reinforcement layout. Based on standard tests conducted on cores and reinforcing bar taken from the bridge, the basic material properties of the bridge were also determined. The average values of the measured initial elastic modulus of concrete and the compressive strength are 23,530 and 23.5 MPa, respectively; the yield stress of the reinforcement bar is 254.8 MPa.

Before full-scale failure test for the bridges, truck load tests were conducted for the span to evaluate load-carrying capacity of the bridges using load and resistance factor methods according to the AASHTO guide and the NCHRP proposal [1,24]. The first target bridge was rated at 1.08 of rating factor, which is equivalent to the load-carrying capacity of DB 14.5 ton (142.1 kN). The second

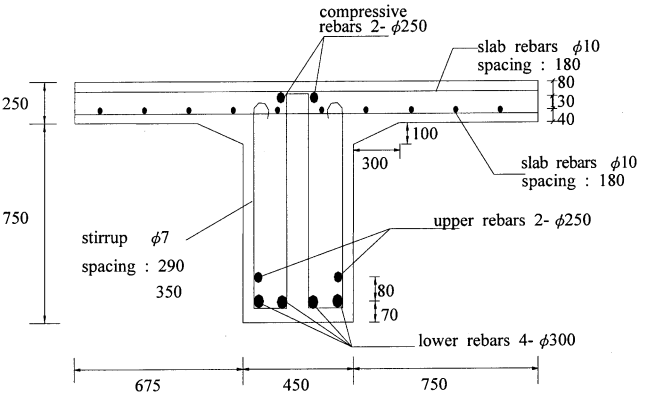

Fig. 2. Reinforcement layout of first target bridge section (unit: mm).

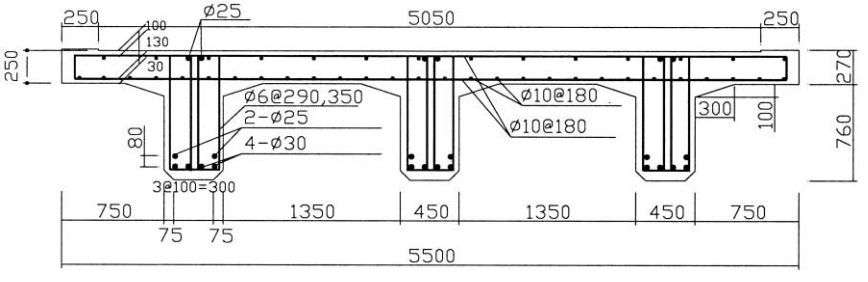

Fig. 1. Dimension of first target RC bridge (unit: mm).

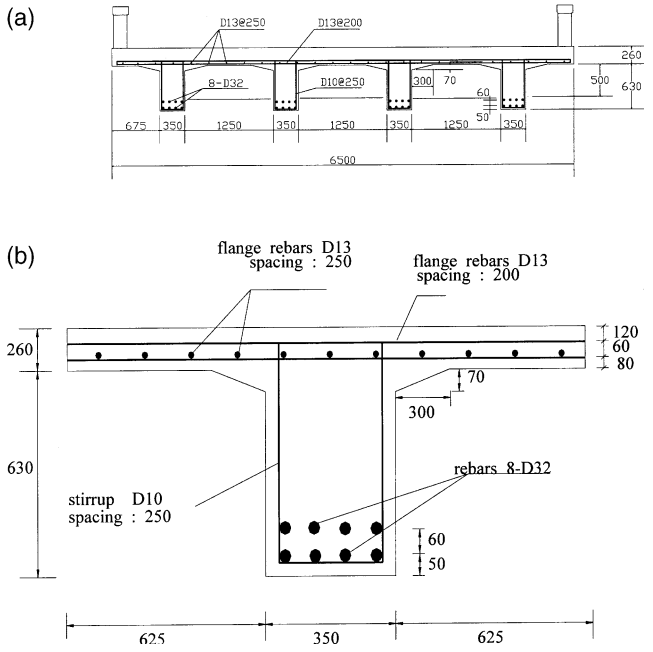

Fig. 3. Second target RC T-girder bridge (unit: mm). (a) Dimension; (b) reinforcement layout.

target bridge was rated at 2.1 equivalent to DB 28.45 ton (278.8 kN).

3. Failure test of target bridges

In order to ignore the stiffening effect of the curbs, which is considerable [7], both curbs and rails of the test spans of the two target bridges were removed before the test and ignored in the analysis too. For the first target bridge, concentric loading at the center of the span is cyclically imposed using two 125-ton (1225 kN) capacity hydraulic jacks arranged along one line at the center of the span so as to simulate a three point bending condition, as shown in Fig. 4. Each jack reacted against a thick steel load cell and the reaction required to load bridge is provided by ground anchors of high-strength pre-stressing tendons passed through a hydraulic jack on an H-shaped steel beam and a timber bed designed to produce uniform pressure on the flange of the girder. Fig. 4 shows details of the test set-up for the first target bridge.

For the second target bridge, cyclic loading was imposed so as to simulate the standard truck loading [1] loaded eccentrically as shown Fig. 5(a). Fig. 5 shows details of the test set-up for the second target bridge.

The test spans were instrumented so that measurements could be made to assess both global and local responses of the bridge. Measurements were made at locations where a maximum response was expected. For several locations along the test spans, deflections of girders were measured using LVDTs; longitudinal strains

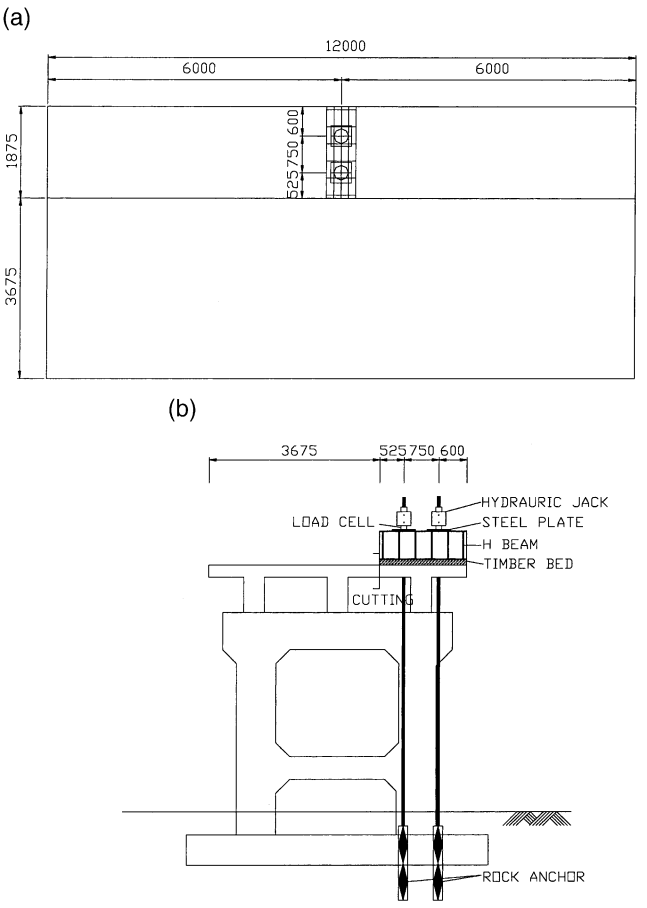

Fig. 4. Test set-up of first target bridge (unit: mm). (a) Plane view; (b) front view.

of the flange concrete and the web concrete of girders flanges were also measured, as were longitudinal strains of bottom longitudinal reinforcing bars in the webs of the girders. Additional measurements like shear strains at the end of spans and crack widths of major cracks during the test were also made. The target bridges were loaded cyclically to failure in approximately equal increments. The load from each hydraulic jacks was controlled to be equal. The initial values for all applicable response measurements were obtained about an hour before application of the first load increment. Loading and unloading in the stage of elastic behavior were repeated to ensure a true initial stiffness of the load–displacement response of the bridges. Then, several cycles of loads were applied up to failure. A set of response measurements was made after each load increment and unloading.

Fig. 6 shows total applied load versus observed deflection at the center of the test span of the first bridge. The response of the bridge up to load 55 ton (539 kN) is almost linear elastic, with no visible damage as a consequence of applied loads. Using the readings from the strain gages attached to the bottom longitudinal bars of the girder, the first yielding of the reinforcing bars

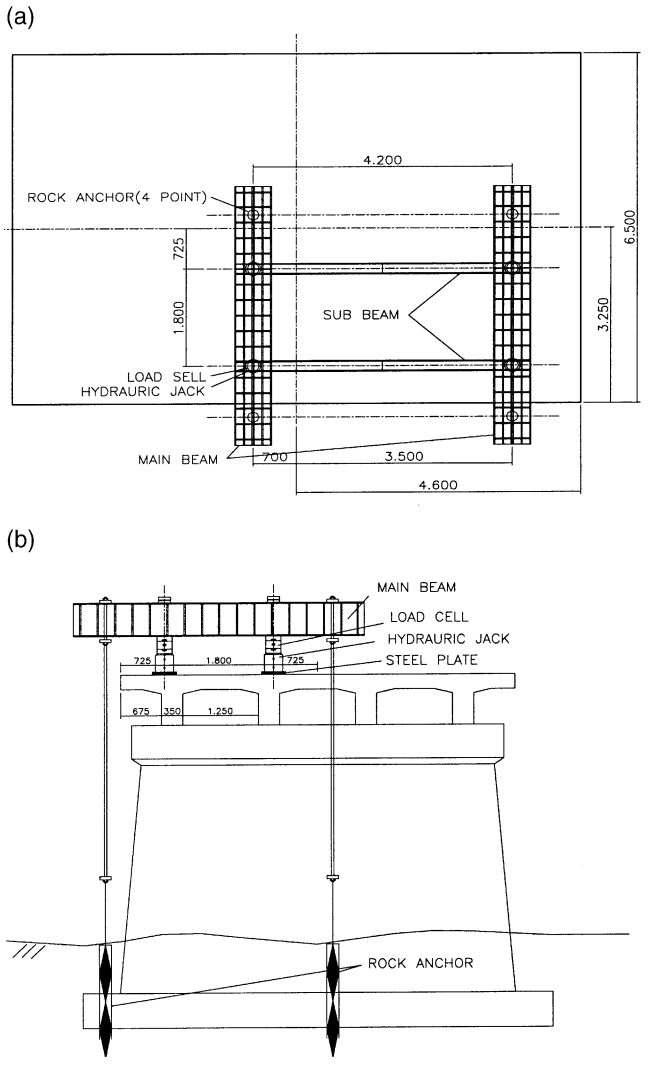

Fig. 5. Test set-up for second target bridge (unit: mm). (a) Plane view; (b) front view.

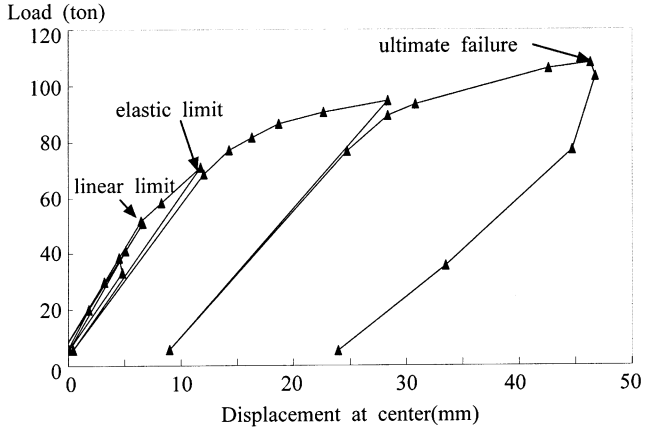

Fig. 6. Total applied load versus deflection response for first target bridge.

was determined to occur when the load on the bridge reached 75 ton (735 kN). Finally, maximum total load by two jacks on the bridge, beyond which no further increase of applied load could be obtained, was 108 ton (1058.4 kN). The obtained maximum load is 1.72 times higher than ultimate load in flexure of 63 ton (617.4 kN) computed analytically according to the ACI 318-95 building code [2]. It is known that the ACI analysis leads to conservative predictions of bridge capacity. One possible reason could be that the materials strength of concrete and reinforcing bars in-situ usually are much larger than the specified nominal values used in design. In order to consider this difference, material properties of the target bridges were measured from concrete cores and reinforcing bars taken from the bridges and were used in the analysis. Another reason is the use of ideal end restraints or support conditions for the analysis of the bridge capacity, which is discussed in detail in Section 5 of this paper.

Fig. 7 shows applied load per jack versus observed deflection at the loading points for all four girders of the second target bridge. As shown in Fig. 7, the response of the second target bridge up to a load of about 30 ton (294 kN) per jack is almost linear elastic and displacement of three girders (G1, G2, and G3) increased non-linearly up to failure, while displacement of the fourth girder (G4) decreased at around 80 ton (784 kN) per jack due to the effect of the eccentric loading condition for this bridge. It is shown that the ultimate load on the bridge reached 412 ton (4037.6 kN) (4 multiplied by 103 ton (1274kN) per jack), which is equivalent to a load carrying capacity of DB 119 ton (1162.2 kN). It is noted that the load carrying capacity obtained using the load and resistance factor methods based on the load test for the second target bridge was DB 28.45 ton (278.8 kN), which is significantly lower than the capacity obtained from the destructive test. It is found that the second target bridge also possesses significantly higher strength than theoretical ultimate strength.

4. Modeling for failure analysis of bridges

A non-linear finite-element analysis technique is applied to develop a computational modeling technique for failure analysis of aged reinforced concrete T-girder bridges that can effectively predict the measured load versus deflection response obtained from the full-scale destructive test of the two target in-situ bridges. An RC zoning method [3,13] is applied to the two-dimensional simple modeling of the symmetrically loaded first target bridge and a combination of fiber model and layered shell model are used for the three-dimensional modeling of non-symmetrically loaded second target bridge. In-plane constitutive laws of average stress and average strain for concrete and reinforcement [18] and a smeared

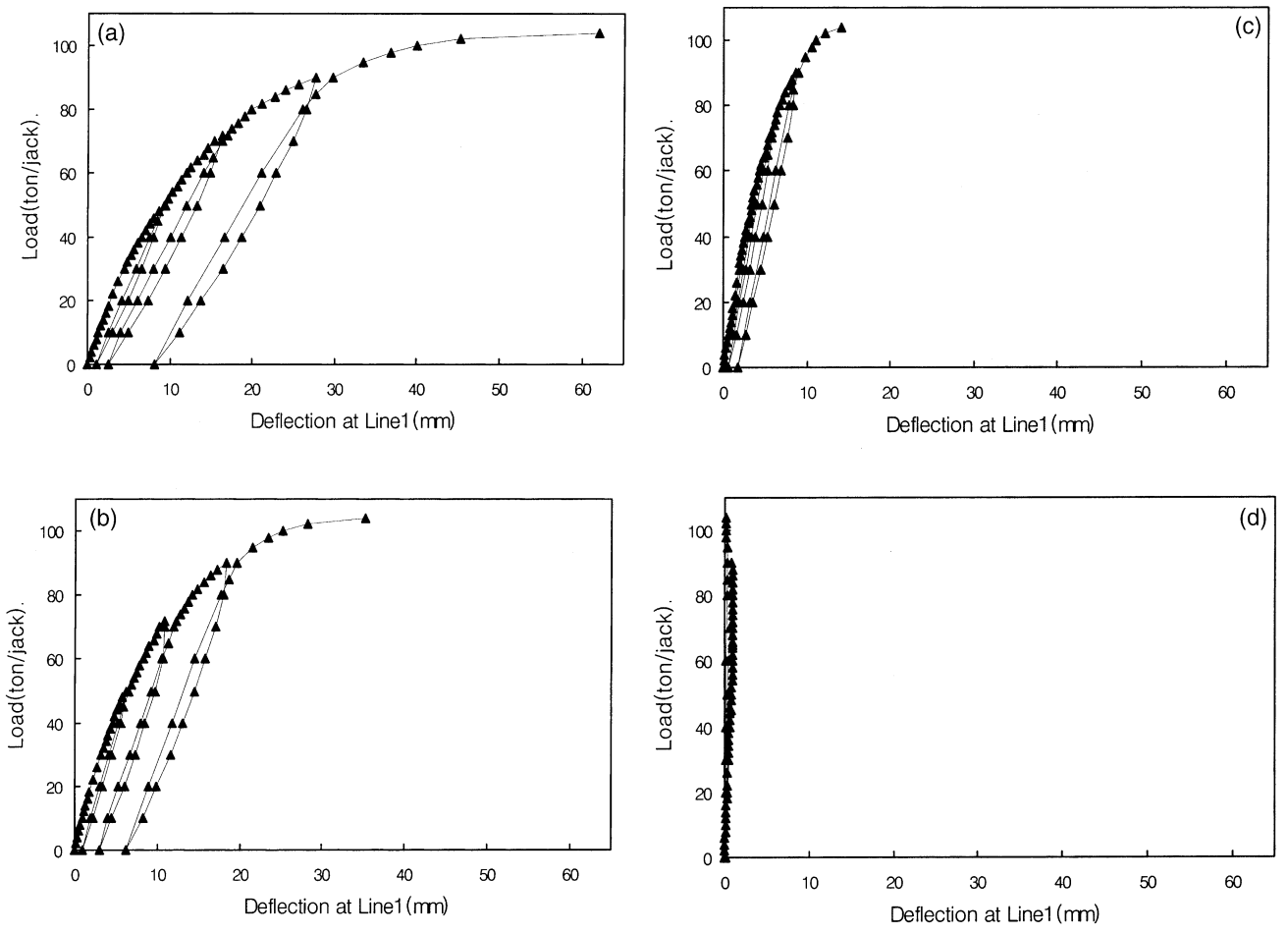

Fig. 7. Applied load versus deflection response for second target bridge. (a) G1 girder; (b) G2 girder; (c) G3 girder; (d) G4 girder.

crack modeling of three-dimensions based on cracked concrete in-plane constitutive laws proposed by Maekawa et al. [14] are utilized for the material modeling. As a first step, monotonic responses of the bridge are computed to identify the effect of support-condition modeling in the failure analysis of an in-situ bridge. Then, a simple modeling technique for the support conditions of the in-situ bridge is proposed. Finally, load versus deflection responses of the test bridges subjected to cyclic loading are computed by applying the aforementioned finite element modeling techniques along with proposed the support-condition modeling and are compared to the measured response.

4.1. Constitutive models of reinforced concrete

In the model for reinforced concrete, a smeared crack model of concrete is employed by combining the constitutive laws, which cover the path-dependant behavior of the loading, unloading and reloading paths, of concrete and reinforcing bars. The cracked concrete model consists of a tension stiffening model [21], a compression model [15], and a shear transfer model [12]. These models are derived from the relationship between average stress and average strain in reinforced concrete, as shown in Fig. 8 [18]. By using the averaged stress–strain relationships, the consistency and uniqueness of the constitutive law independent of size of crack spacing, crack density and diameter of reinforcing bars can be obtained [19]. Prior to cracking, concrete is modeled as an elasto-plastic and fracture (EPF) material [15,16]. The EPF model idealizes mechanical behaviors of un-cracked concrete as combined plasticity and continuum fracture that identifies induced permanent deformations and loss of elastic strain energy absorption capacity, respectively. In the model, concrete is considered as an infinitesimal elasto-plastic component. Concrete elasticity is modeled as springs while the concrete plasticity is modeled as sliders. The damage inside the concrete is modeled as broken springs. Total stress is identified as the assembly of internal stresses developing over active non-damaged elasto-plastic components. Elastic strain is chosen to represent the internal stress intensity that governs the plasticity and fracturing in the concrete continuum defects. Non-linearity of the pre-cracking concrete due to the fracture and plasticity is again distinguished in volu-

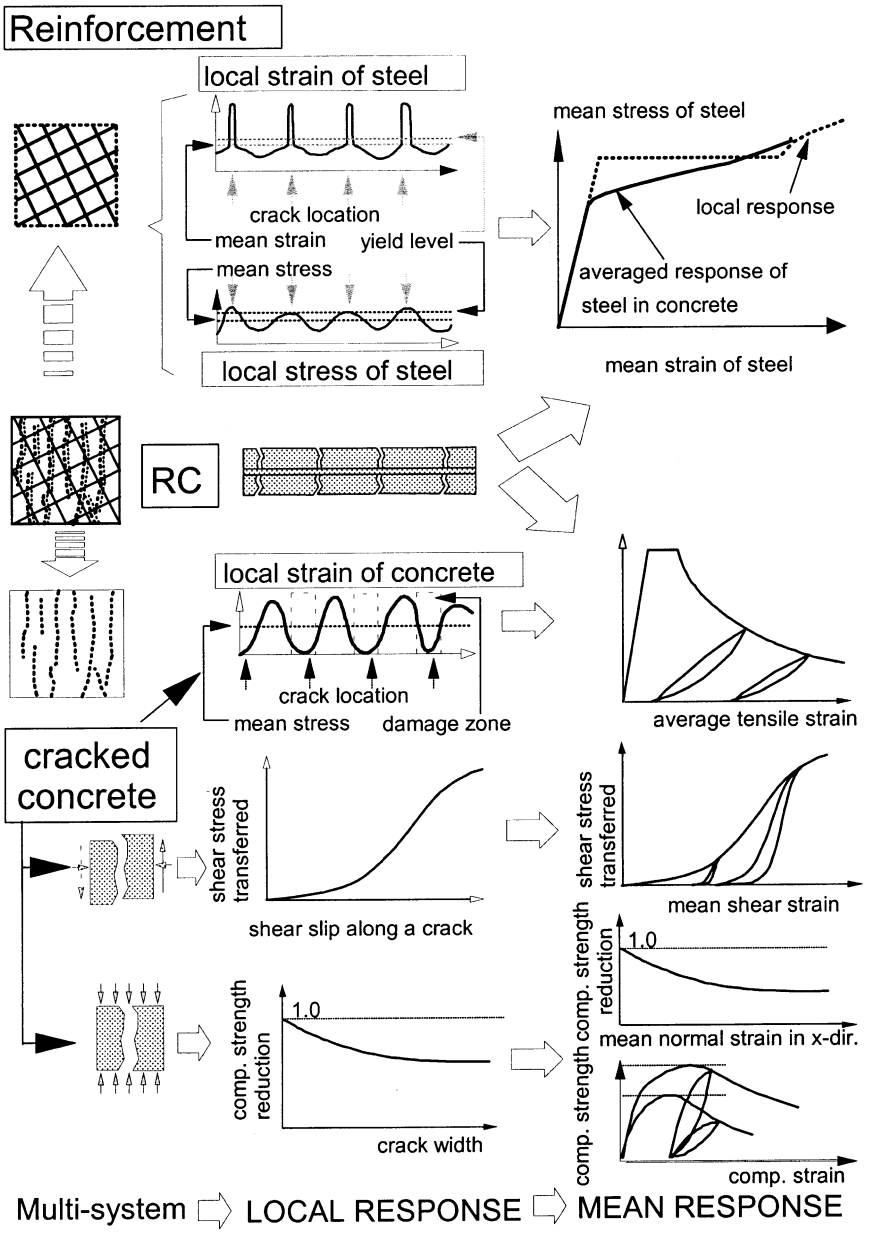

Fig. 8. Constitutive models of reinforced concrete.

metric and deviatoric mode in formulation [16]. By considering localization of the plastic strains of reinforcing bars inside the cracked concrete at post-yield range, the modeling of reinforcing bars is also given in the form of average stress versus average strain in a bilinear line [22] as shown in the Fig. 8. For calculating the mechanical behaviors of reinforcing bars in concrete under cyclic loadings, Kato's model [11] for a bare bar under reversed cyclic loading with the assumption of stress distribution denoted by a cosine curve is used. It should be noted that the combination of all these constitutive models provides a fully path dependent and cyclic averaged stress–strain relationship that can simulate any arbitrary paths including loading, unloading and reloading conditions, and that they are verified at element and member levels [18,19].

For large concrete beams where reinforcing bars are located at the bottom of beams and the reinforcement ratio is very small, some volume of concrete is outside the RC control volume in which tensile stress is not transferred through the bond mechanism with reinforcement. The spatially averaged mechanical property of concrete distant from the reinforcing bars is different from that of concrete surrounding the reinforcing bars because the bond effect decreases as the distance from the reinforcing bars increases. The behavior of concrete outside the bond-effective zone is supposed to be the same as that of plain concrete, showing sharp strain-

softening features as the tensile stress is transmitted through a bridging action at the crack surface, but the concrete confined by reinforcing bars shows stiffening behavior, i.e. stable stress release after cracks for either tension or shear owing to the bond. The cracked reinforced concrete model illustrated in Fig. 8 can only be applied to cracked concrete near the reinforcement. A modified cracked concrete model for the plain concrete zone far from the RC control volume of reinforced concrete [13] is used in our analysis. As shown in Fig. 9, once cracks are generated in concrete, respectively, for the plain concrete zone and the RC zone, tension softening and tension stiffening stress–strain relations are applied in the directions normal to the cracks and shear softening and shear stiffening models are applied in the shear direction parallel to the cracks. These shear transfer models are based on the contact density function of Li et al. [12].

4.2. Finite element modeling

In finite element computations of real scale reinforced concrete structures such as the target bridges, larger finite elements must sometimes be used due to limitations on the number of finite elements and restricted computational capacity. Then, some volume zoning concept for the finite elements is necessary to correctly detect distinct average constitutive laws of concrete close to and far from reinforcement and to consider spatial orientations of the bond effect on concrete; in other words, it becomes clear that a rational method is desired to determine the size of the RC zone. A simple engineering method called the RC zoning method, based on a single bar equilibrium condition, was proposed by An et al. [3]. The RC zone for a single reinforcement bar is determined on condition that the tension force carried by the RC zone concrete just prior to cracking must be equal to the yield force which the reinforcing bar can support at maximum through the bond mechanism after cracking. The RC zoning method is utilized for finite element modelings of the target bridges by considering two different zones in the finite element discretization of bridge sections: the RC zone and the plain concrete zone (PL zone) outside the RC zone.

For two-dimensional finite element modeling of the first target bridge, different widths of the flange and the web of the girder were considered and the height of the RC zone was determined by the diameter of each reinforcement bar based on the RC zoning method. The overlapping RC zone of neighboring reinforcing bars as well as the part of the RC-zone that falls outside the bridge boundary was not taken into account. Fig. 10 shows two-dimensional modeling of the first target bridge along with a spring attached to the roller support, which will be proposed support modeling for aged bridges later in this paper. It can be seen that the finite elements of the section of the first target bridge are divided into both RC zones, shown as shaded elements in the figure, and PL zones. Since the top reinforcing bars in the flange are very small and the modified height of the RC zone becomes too small for finite-element discretization, it can be ignored in the modeling, even though the situation where one element contains both RC zones and PL zones can be considered in the modeling [3].

For the second target bridge loaded eccentrically, full three-dimensional modeling for the entire bridge is necessary because the three-dimensional response of a bridge due to the loading condition can not be simulated with the two-dimensional modeling. The combination of frame elements and multi-layered shell elements was used for the three-dimensional modeling of the second target bridge. Both longitudinal and transverse girders were modeled by the frame elements, which are analyzed by fiber technique and the zoning method, while slabs on the girders were modeled by the multi-layered shell elements.

In the fiber technique [17,23,25,26], each element is represented using a single line coinciding with the centerline of the member. The member cross-section is divided into many cells or sub-elements as shown in Fig.

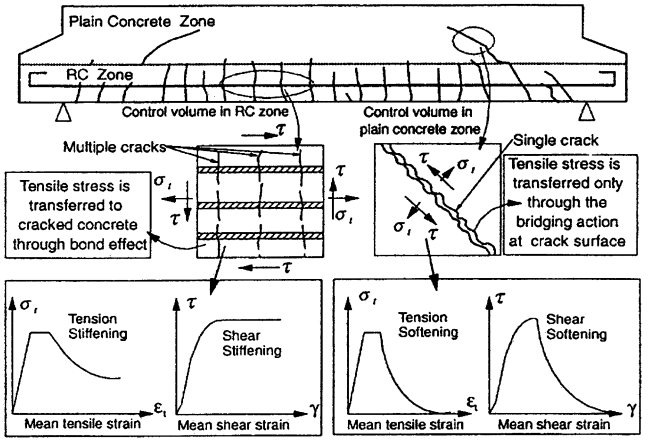

Fig. 9. Responses of concrete near and far from reinforcement.

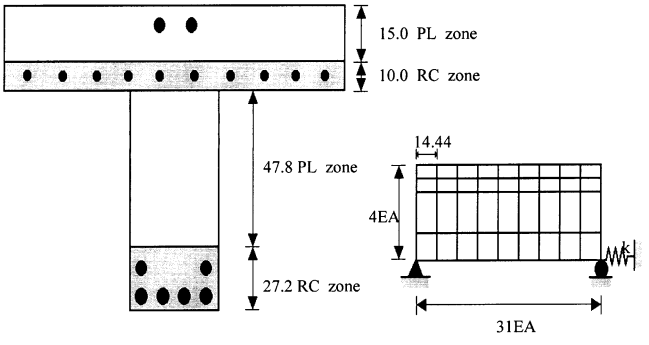

Fig. 10. 2D finite element modeling of first target bridge (unit: cm).

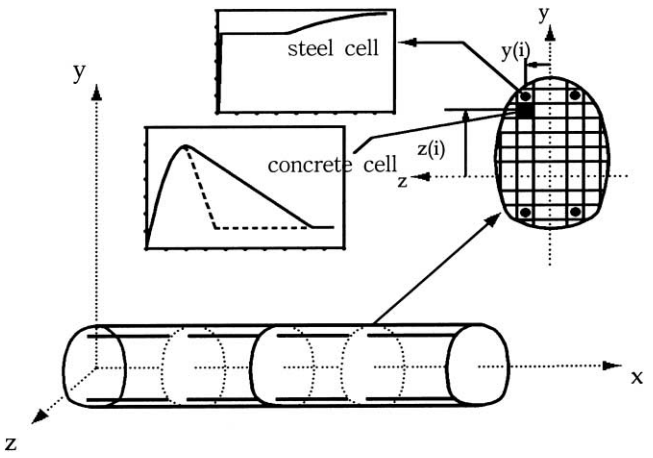

Fig. 11. Frame element with fiber technique.

11. The strain of each cell is calculated based on Euler–Kirchoffs hypothesis, i.e. plane section remains plane after bending. For each fiber strain along the axis of a finite element, the response is calculated using the aforementioned material constitutive models representing the local behavior. Similarly, the concrete cells in the cross-section are divided into two categories according to distance from the steel cells. Concrete cells closer to the reinforcement are modeled as RC zone and those far from the reinforcement are modeled as PL zone. The overall response of each element is the integrated response of these fibers and the overall response of the member comprises all the element responses.

For modeling the slabs on girders of the second target bridge, an eight-node degenerated shell element was used; the shell element was divided into several layers of panel where the aforementioned constitutive models were applied to each layer of the shell to take into account material non-linearity [10]. Each layer was classified as a plain concrete layer or reinforced concrete layer reached by the bond so that the cracking behavior was controlled by reinforcing bars being smeared in the layer and the steel layer (Fig. 12). Since a certain amount of cracked concrete surrounding a reinforcing bar contributes to the stiffness of the element, the whole volume of concrete is considered to contribute to the tension stiffness of the element so that there is a tension softening effect even inside the plain concrete layer. Each layer contains stress points on its mid-surface. The stress components of the layer are computed at these stress points and are assumed to be constant over the thickness of each layer, so that the actual stress distribution of the shell is modeled by a piecewise constant approximation. A mid-point integration rule is applied for each layer. Fig. 13 shows the details of the finite element modeling for the target bridge.

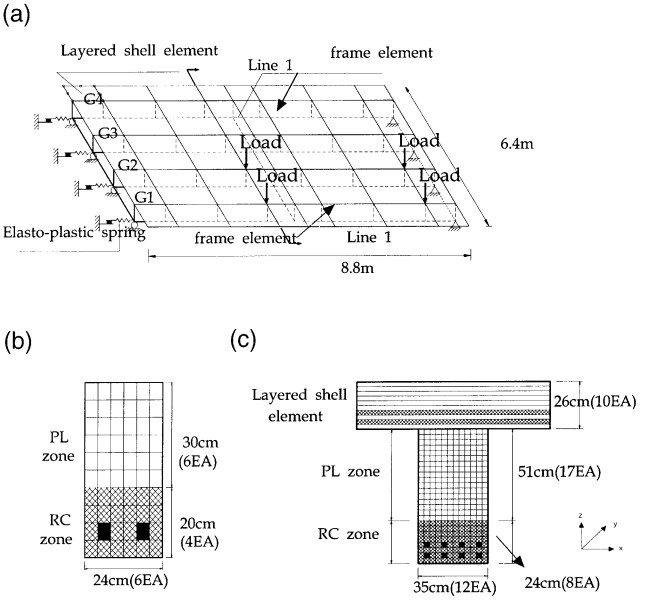

Fig. 13. Three-dimensional modeling of second target bridge. (a) Finite elements used for modeling; (b) discretization of transverse girder; (c) discretization of slab with longitudinal girder.

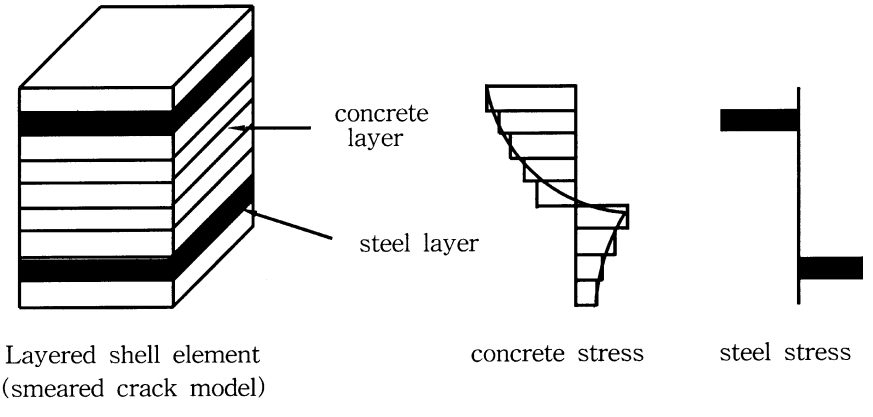

Fig. 12. Layered shell element.

5. Failure analysis and comparisons

As a first step in failure analysis, monotonic responses of target bridges are computed to identify the effect of support-condition modeling in the failure analysis of the target bridges. Then, a modeling technique for the degraded support conditions in in-situ aged bridges is applied. Finally, total load versus deflection responses of the target bridges subjected to cyclic loading are computed by finite element analysis with the proposed support-condition modeling technique and results are compared to the measured responses. The effect of support modeling in non-linear finite element analysis for aged reinforced concrete slab bridges was also found to be significant [8,20]. Only the upper and lower bounds of global responses can be computed from the idealized support conditions. In order to model the support conditions of the in-situ target bridges, a simple modification of support condition is proposed by assuming the rotational friction at the supports of the target bridges to be small enough and by attaching a horizontal spring to the roller supports of the bridges, as shown in Figs. 10 and 13. Then, a spring stiffness constant of the proposed spring is obtained from calibration with the initial stiffness of the load–deflection curve of the target bridge obtained from a service load test. For the first target bridge, the spring constant k=600 kN/mm was obtained by calibrating the initial stiffness of the computed response to that of the measured response. A spring constant k=1470 kN/mm for a horizontal elastic spring attached to the roller support at each girder was also obtained for the second target bridge. In order to reflect the inelastic behavior of the second target bridge, which starts with the yielding of the tension reinforcing bars located at the bottom of the girders of the bridge, the support spring for the second target bridge is assumed to commence perfectly plastic behavior upon the yielding of reinforcing bars. Three separate analyses were carried out with different support conditions: hinge support condition assuming that all the supports at the piers are hinge supports, simple support condition (one end a hinge, the other a roller) and the proposed support condition with the spring. Fig. 14 shows that the predicted responses of the first target bridge were substantially different from the measured response and were significantly affected by the choice of the support condition modeling of the in-situ bridge. Fig. 14 also shows that the computed response with the proposed modeling for support condition of first target bridge was in good agreement with the test result. Only the upper and the lower bounds of global responses can be computed from the idealized support conditions.

As shown in Fig. 15, predicted responses for the second target bridge using the idealized support modeling in the analysis are also substantially different from the measured responses and the simple proposed modeling for support can be used effectively for the failure analysis of aged reinforced concrete bridges.

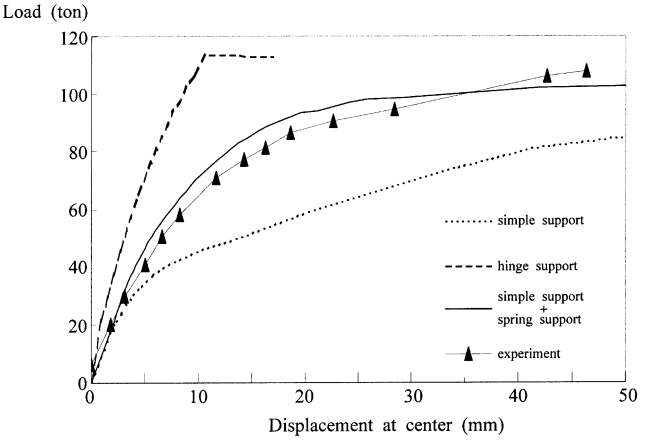

Fig. 14. Computed responses for different support conditions.

The experimental data used to calibrate the horizontal spring are usually not available. In such cases, even powerful computation tools for the failure analyses of reinforced concrete bridges only provide the upper and lower bounds of strength and stiffness of in-situ bridge, which are substantially different from the real behaviors of the bridge. However, non-destructive tests for in-situ bridges, such as the tests used for rating old bridges [4,5,8], to obtain the initial stiffness of the load–deflection response of the bridges can be done more easily than full-scale failure tests, and the initial stiffness of the response is only experimental data for the proposed modeling technique for the support conditions of in-situ bridge. Shahrooz et al. [20] used a number of linear rotational springs placed at each abutment for the boundary condition modeling of a deteriorated reinforced concrete slab bridge, which was connected to abutments by shear keys, and spring stiffness constants were identified such that the measured and computed responses of the bridge matched closely.

Figs. 16 and 17 show computed load–deflection response modeled with the proposed modeling for the support condition of the target bridges subjected to cyclic loading. Comparison with the measured response shows that the finite-element modeling techniques for in-situ bridges with the proposed modeling technique for the support condition are fairly good for the failure analysis of reinforced concrete T-girder old bridges subjected to cyclic loading.

6. Conclusion

For two in-situ aged reinforced concrete T-girder bridges, full-scale destructive tests have been performed by applying cyclic loads up to failure to observe the failure behaviors of the bridges experimentally and finite

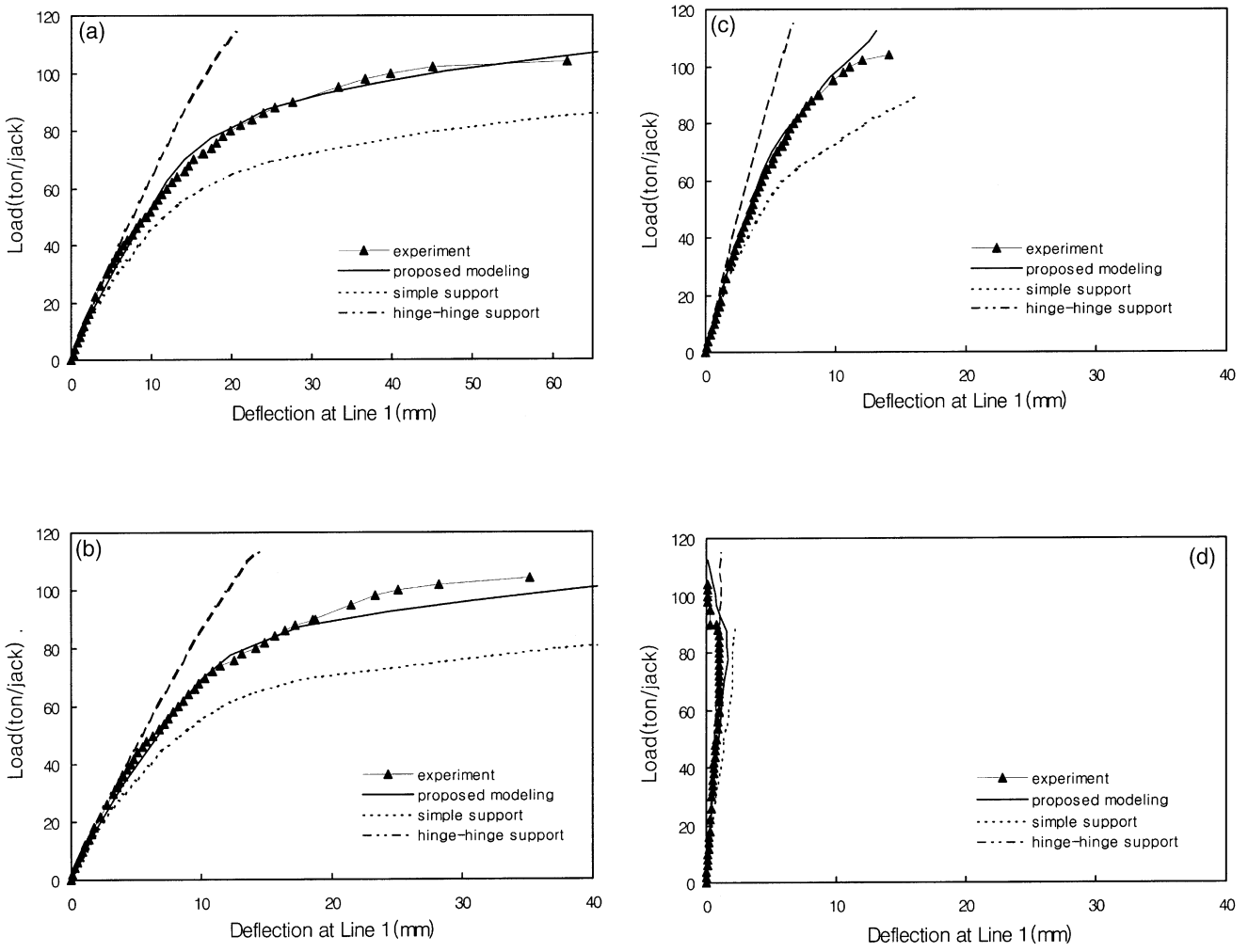

Fig. 15. Computed responses for different support conditions of second target bridge. (a) G1 girder; (b) G2 girder; (c) G3 girder; (d) G4 girder.

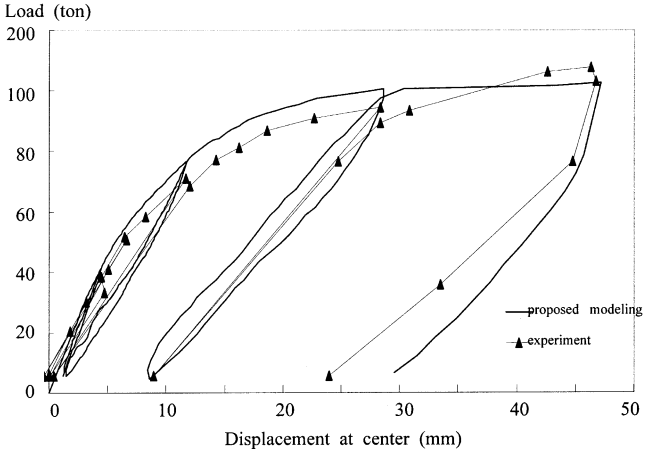

Fig. 16. Responses of first target bridge subjected to cyclic loading.

element analyses have been carried out to predict their behaviors analytically. Experimental results indicate that significant load carrying capacity is retained in old reinforced concrete bridges and analysis results show that modeling of the degraded support conditions of the bridges significantly affects the predicted responses of the capacity as well as the stiffness of the bridges. A modeling technique for the support conditions of old bridges has been proposed and has proved to be effective for the failure analysis of in-situ bridges. Two and three-dimensional finite element modeling techniques along with the proposed support condition are applied to modeling of the bridges for failure analysis by utilizing path-dependent in-plane constitutive laws of cracked reinforced concrete and zoning method. Analytical results and comparisons with the experimental results show that the finite element analysis techniques in this paper can be effectively applied to the failure analysis of in-situ deteriorated reinforced concrete T-girder bridges subjected to cyclic loading.

Acknowledgements

The financial support by a fund of Korea Infrastructure Safety and Technology Corporation in Korea for

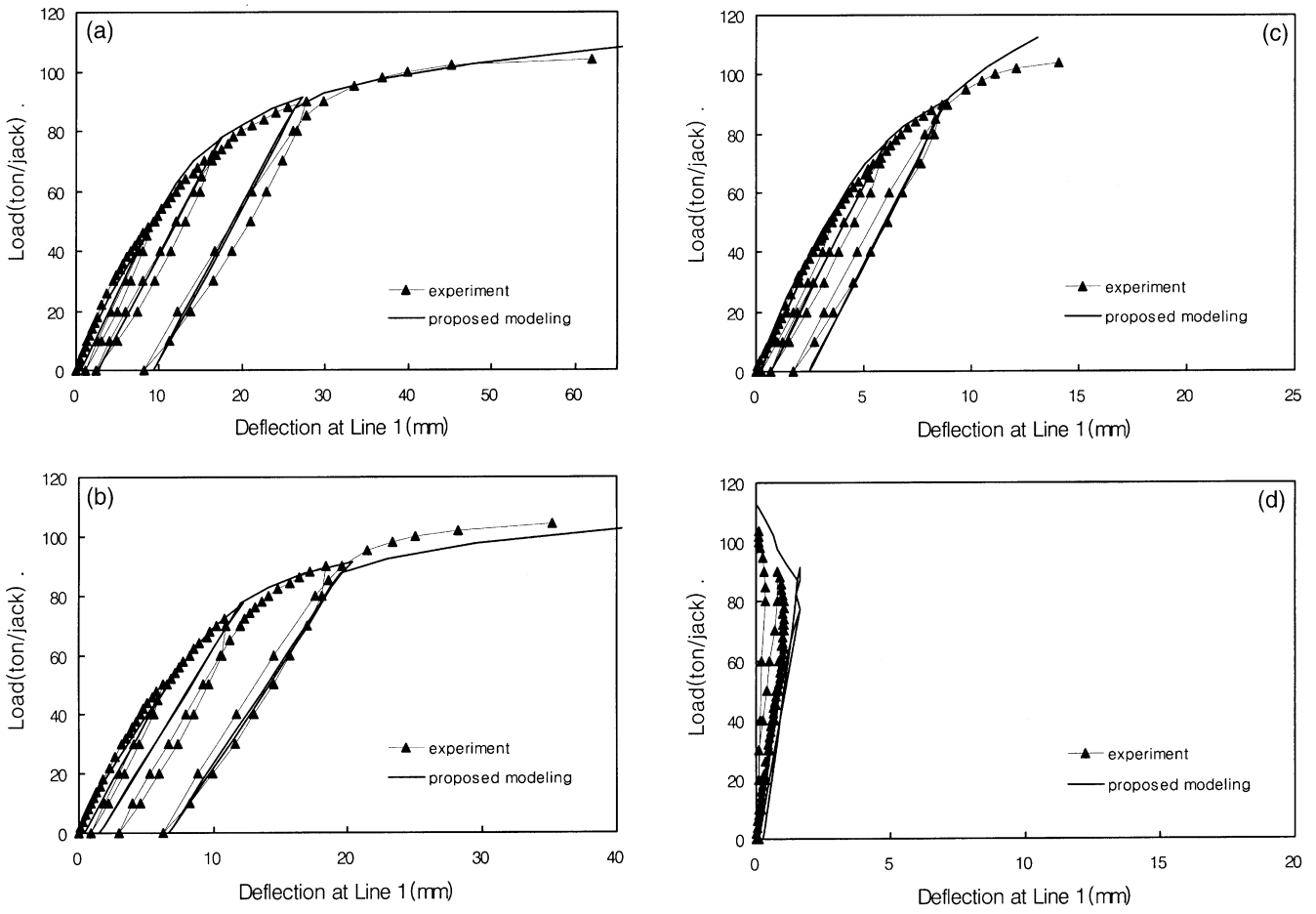

Fig. 17. Responses of second target bridge subjected to cyclic loading. (a) G1 girder; (b) G2 girder; (c) G3 girder; (d) G4 girder.

this research is gratefully appreciated. The support of the Yonsei University and the University of Tokyo to the first author is also gratefully acknowledged.

References

[1] AASHTO. Guide specifications for strength evaluation of existing steel and concrete bridges. Washington DC: AASHTO, 1989.
[2] ACI Committee 318. ACI318-95, building code requirements for reinforced concrete. Redford Station, Detroit (MI): ACI, 1995.
[3] An X, Maekawa K, Okamura H. Numerical simulation of size effect in shear strength of RC beams. J Mater, Concrete Struct Pavements 1997;35(564):297–316.
[4] Azizinamini A, Boothby TE, Shekar Y, Barnhill G. Old concrete slab bridges. I: Experimental investigation. J Struct Eng, ASCE 1994;120(11):3284–304.
[5] Azizinamini A, Shekar Y, Boothby TE, Barnhill G. Old concrete slab bridges. II: Analysis. J Struct Eng, ASCE 1994;120(11):3305–19.
[6] Bhkht B, Jaeger LG. Bridge testing — a surprise every time. J Struct Eng 1990;116(5):1370–83.
[7] Ho I, Shahrooz BM. Finite element modeling of a deteriorated R.C. slab bridge: lessons learned and recommendation. Struct Eng Mech 1998;6(3):259–74.
[8] Huria V, Lee K-L, Aktan AE. Different approaches to rating slab bridges. J Struct Eng 1994;120(10):3056–62.
[9] Huria V, Lee K-L, Aktan AE. Nonlinear finite element analysis of RC slab bridge. J Struct Eng 1992;119(1):88–107.
[10] Irawan P. Three dimensional analysis of reinforced concrete structures. Doctoral dissertation, University of Tokyo, 1995.
[11] Kato B. Mechanical properties of steel under load cycles idealizing seismic action. CEB Bull Informat 1979;131:7–27.
[12] Li B, Maekawa K, Okamura H. Contact density model for stress transfer across cracks in concrete. J Faculty Eng, Univ Tokyo (B) 1989;40(1):9–52.
[13] Maekawa K, An X. Shear failure and ductility of RC columns after yielding of main reinforcement. In: Engineering fracture mechanics, vol. 65. New York: Pergamon, 2000.
[14] Maekawa K, Irawan P, Okamura H. Path-dependent three-dimensional constitutive laws of reinforced concrete formulation and experimental verifications. Struct Eng Mech 1997;5(6):743–3.
[15] Maekawa K, Okamura H. The deformational behavior and constitutive equation of concrete using elasto-plastic and fracture model. J Faculty Eng, Univ Tokyo (B) 1983;37(2):253–328.
[16] Maekawa K, Takemura J, Irawan P, Irie M. Triaxial elasto-plastic and continuum fracture model for concrete. Concrete Library, JSCE 1993;22:131–61.
[17] Menegotto M, Pinto PE. Method of analysis of cyclically loaded RC plane frames including changes in geometry and non-elastic behavior of elements under normal force and bending. Preliminary report, IABSE, no. 13, 1973:15–22.
[18] Okamura H, Maekawa K. Nonlinear analysis and constitutive model in reinforced concrete. Tokyo: Gihodo-Shuppan Co, 1991.
[19] Okamura H, Maekawa K. Reinforced concrete design and size

effect in structural nonlinearity. In: Invited paper of Proceeding of JCI International Workshop on Size Effect of Reinforced Concrete Structures, Sendai (Japan), 1993:1–20.
[20] Shahrooz BM, Ho IK, Aktan AE, de Bost R, van der Veen, Iding RH, Miller RA. Nonlinear finite element analysis of deteriorated RC slab bridge. J Struct Eng 1994;120(2):422–39.
[21] Shima H, Chou L, Okamura H. Micro and macro models for bond behaviour in reinforced concrete. J Faculty Eng, Univ Tokyo (B) 1987;39(2):133–94.
[22] Shima H, Tami S. Tension stiffness model under reversed loading including post yield range. In: IABSE Colloquium, Delft, 1987:547–56.
[23] Taucer F, Spacone E, Filippou FC. A fiber beam-column element for seismic response analysis of reinforced concrete structures. EERC Report 91-17, University of California, Berkeley: EERC, 1991.
[24] TRB. Strength evaluation of existing reinforced concrete bridges. Washington DC: Transportation Research Board, National Research Council, 1987.
[25] Zeris CA, Mahin SA. Analysis of reinforced concrete beam-columns under uniaxial excitation. J Struct Eng, ASCE 1988;114(ST4):804–20.
[26] Zeris CA, Mahin SA. Behavior of reinforced concrete structures subjected to biaxial excitation. J Struct Eng, ASCE 1991;117(ST9):2657–73.